

their wide applications in many fields, especially in the industrial and biological fields⁸. Azo dyes are created by diazotizing aromatic or heteroaromatic primary amines, then coupling the resultant diazonium ion to an electron-rich nucleophilic compound. Aqueous mineral acids like hydrochloric acid and sodium nitrite (NaNO_2) are typically combined to create HNO_2 nitrous acid at $0 - 5^\circ \text{C}$. The nitrous acid forms an N-nitroso intermediately by combining with aromatic amines, which it then tautomerizes into a diazo hydroxide. The diazonium ion is produced via protonation of the hydroxyl group and water elimination⁹⁻¹¹. The present work prepared

new azo ligand and a series of complexes by using Ni,(II), Pd,(II), Pt(IV) and Au(III) which were examined by ^1H & ^{13}C -NMR spectra, Mass spectra, FT-IR, UV-vis spectroscopy and (TGA&DSC) curves, as well as chloride and metal contents, element micro analysis, magnetic moment measurements, molar conductance. The DCS curve was used to calculate the thermodynamic parameters ΔH , ΔS and ΔG , then antioxidant activity of these compounds was studied and determined against the DPPH radical (1,1-diphenyl-2-picrylhydrazyl) and compared to that of a standard natural antioxidant Gallic acid.

Materials and Methods

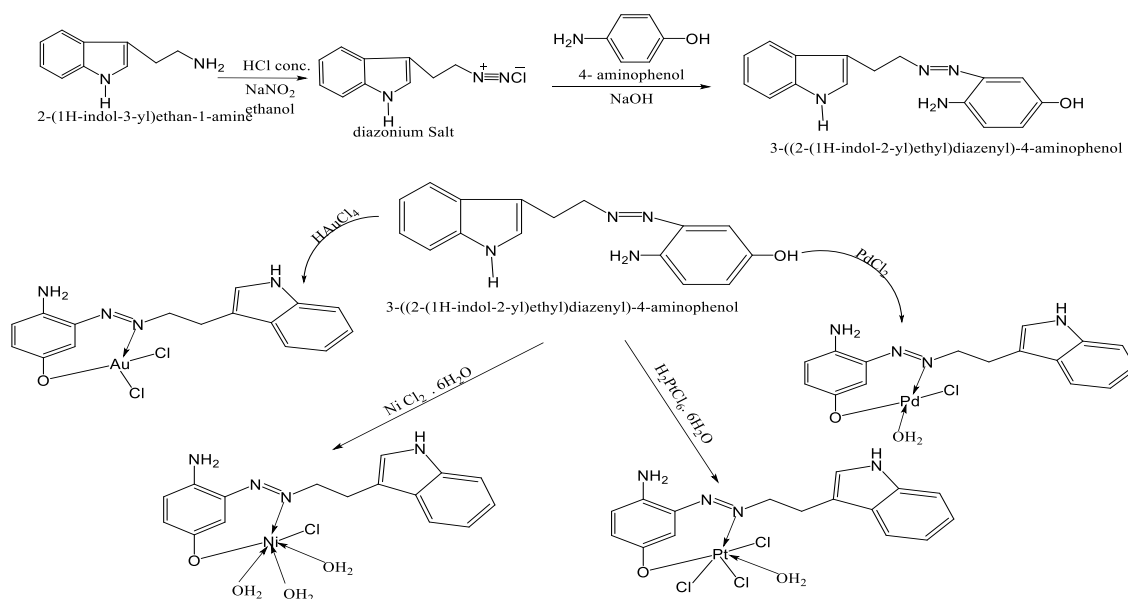
All chemical components came from sources that (Sigma-Aldrich, Merck, and others). All organic solvents were readily available in the marketplace and were properly distilled and dried. The Bruker (500MHz) Spectrometer was used to obtain the ^1H and ^{13}C NMR spectra. ^1H and ^{13}C NMR spectra were obtained from Bruker (500MHz) spectrometer. The UV-visible absorption spectra were obtained using a UV-1800 Shimadzu spectrophotometer. The QP50A: DI Analysis ShimadzuQP-2010-Plus (E170Ev) spectrometer was used to measure mass spectra. IR spectra were measured by IR Prestige-21. Euro vector model EA/3000, Single-V.3.O-single was utilized to obtain (C, H and N) elemental analyses. Utilizing a Shimadzu (A.A) 680 G atomic clock, metals were identified. A conductometer WTW was used to detect conductivity while it was at room temperature with DMSO solutions. On QP50A: DI Analysis ShimadzuQP-2010-Plus (E170Ev) spectrometer, electron impact (70 eV) mass spectra were captured. A gravimetric estimation of the chloride concentration was made. The balancing magnetic susceptibility model MSR-MKI was utilized magnetic characteristics. Perkin-Elmer Pyris Diamond DS/TGA was used for all prior sorts of thermal analysis.

Synthesis of Azo Ligand (H_2L)

Tryptamine (0.25 g, 0.003 mol) was dissolved in 2 mL hydrochloric acid, then was cooled to $0-5^\circ \text{C}$. The aforementioned cold mixture was thoroughly stirred before adding a solution of sodium nitrite (10%, 0.43 g, 0.006 mol) in 15 mL of distilled water. The completion of the diazotization after 30 minutes was determined by introducing a solution of (0.34 g, 0.003 mol) of 4-aminophenol. The final result, which had turned dark brown, was filtered, dried, gathered, and weighed. The yield was 66%, and the melting point was between $152-155^\circ \text{C}$ ¹².

Synthesis of Metal Complexes

A metal salt solution of 1 mmol [$\text{NiCl}_2 \cdot 6\text{H}_2\text{O}$ (0.23g), PdCl_2 (0.19g.), $\text{H}_2\text{PtCl}_6 \cdot 6\text{H}_2\text{O}$ (0.37g) HAuCl_4 (0.37g.)] were dissolved in 10ml of ethanol, then 0.31 g, 1mmole of ligand (H_2L) solution was dissolved in 10 ml for ethanol. At $50-70^\circ \text{C}$, the mixture was refluxed for two hours. After filtering out any remaining unreacted components with small volumes of hot ethanol, the precipitates were dried, and collected, then weighed. The following scheme 1 shows the preparation of the ligand (H_2L) and its metal complexes.



Scheme 1. Formation of ligand(H₂L) and their metal complexes

The Antioxidant Activity by DPPH Method

100 μL of each sample solution at different concentration (0.2, 0.4, 0.6, 0.8 and 1 mmol⁻¹) were mixed with 6 ml of a DPPH ethanolic solution 45 μg/ml. After 30, 60 minutes reaction period was done at room temperature in dark place. Then DPPH interacted with an antioxidant substance that has the ability to donate hydrogen. The color shifted (from deep violet to light yellow). The absorbance was measured against at 517 nm by using a UV-Visible

spectrophotometer. The equation used to calculate percentage of DPPH radical scavenger is:

$$\text{DPPH scavenging ability (\%)} = \frac{\text{Abs control} - \text{Abs sample}}{\text{Abs control}} \times 100 \dots \dots 1$$

Gallic acid was utilized as a reference for a variety of substances, including ligand (H₂L₁) and solutions for their metal complexes, ligand (H₂L₂) and solutions for their metal complexes, and ligand (H₂L₃) and solutions for their metal complexes

Results and Discussion

Physical and Analytical Data for Ligand(H₂L) and the Synthesized Complexes

Table 1 shows the physical and some analytical data for the ligand and their generated complexes, including melting temperatures, colors,

elemental analyses, yield and metal percentages. The results from the experiment matched those from the estimates, and both the chloride and metal contents lead to the metal salts were amount of [1:1] ratio of [M:L].

Table 1. Analytical information of ligand (H₂L) and their metal complexes

Compound	Formula M.wt	%M (Expert) Calc	%Cl (Expert) Calc	(Expert) Calc				Color	Yield %	m.p °C
				%C	%H	%N	%O			
H ₂ L	C ₁₆ H ₁₆ N ₄ O 280.32	-	-	(67.87) 67.84	(5.63) 6.71	(21.13) 19.78	(5.41) 5.67	dark brown	71	150- 152
[Ni(H ₂ L)(H ₂ O) ₃ Cl]	C ₁₆ H ₂₁ N ₄ NiO ₄ Cl 427.14	(14.04) 13.81	(7.89) 8.29	(45.08) 44.91	(3.79) 4.91	(14.41) 13.11	(14.81) 14.97	green	68	d272- 273
[Pd(H ₂ L)(H ₂ O)Cl]	C ₁₆ H ₁₇ N ₄ O ₂ PdCl 438.87	(25.01) 24.24	(7.66) 8.07	(42.89) 43.74	(4.09) 3.87	(13.05) 12.76	(7.86) 7.29	reddish brown	66	d230- 233
[Pt(H ₂ L)(H ₂ O)Cl ₃]	C ₁₆ H ₁₇ N ₄ PtO ₂ Cl ₃ 598.44	(33.01) 32.59	(17.96) 17.76	(33.07) 32.09	(2.52) 2.86	(10.00) 9.36	(5.95) 5.34	pink	70	d120- 122
[Au(H ₂ L)Cl ₂]	C ₁₆ H ₁₅ AuCl ₂ N ₄ O 546.863	(35.01) 36.00	(13.06) 12.96	(34.65) 35.10	(2.96) 2.74	(11.67) 10.24	(3.06) 2.92	gray	62	d139- 141

Calc=calculated, d= decompose

¹H-NMR spectra for Ligand (H₂L):

The ¹H-NMR spectrum of ligand (H₂L) ¹³ can be seen in Fig 1 and Table 2.

Table 2. ¹H-NMR spectral data of ligand (H₂L)

Chemical shift δ(ppm)	Functional Group
1.5-2.0	((4H)t,CH ₂ -CH ₂)
2.50	DMSO
6.94	((1H)s,CH-NH _{Indole})
6.76	((1H)d,CH-OH)
7.58-7.60	((1H) d,CH-NH ₂)
7.83-7.86	((1H)s, CH-N=N)
7.96-8.0	((4,H)m, CH _{arom})
9.5	((2H,) s,NH ₂)
10.5	((1H), s,OH)
11.30	((1H), s,NH)

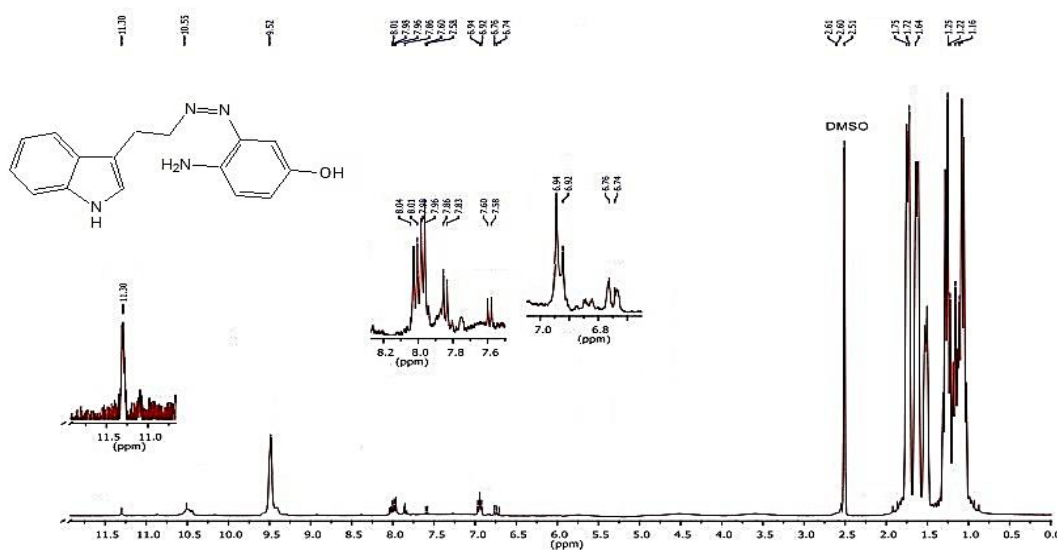


Figure 1. ¹H-NMR spectrum for ligand (H₂L)

¹³C-NMR Spectra for Ligand (H₂L):

The ¹³CNMR Spectra of ligand (H₂L) revealed multiple chemical shifts. (C1:134.11, C2:125.34, C3:180.02, C4: 106.3,C5:175,

C6:168.72, C7:49.31, C8:35.51, C9:122.5, C10:166.12, C11:148.5, C12:150 and C13:139.4) to the carbon atoms respectively¹⁴. Fig 2 shows the ¹³CNMR for ligand (H₂L).

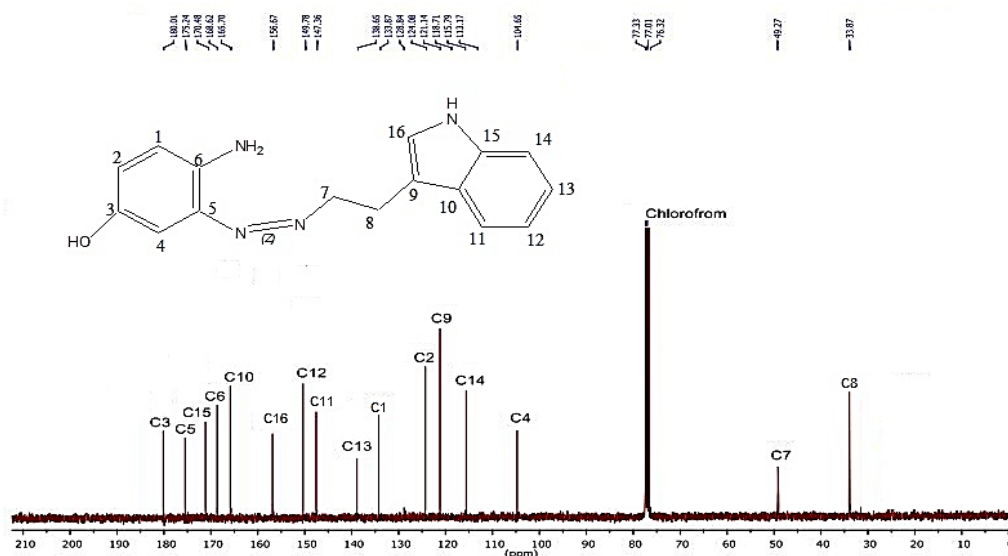


Figure 2. ¹³C-NMR spectrum of ligand (H₂L)

(LC-MS) Measurements

The mass spectrum for ligand(H₂L) and their synthesized complexes show a good defined the parent peak and fragmentation ion pattern. Fig 3 displays the mass spectrum of the ligand (H₂L). The pattern of fragmentation is summarized in scheme 2. The molecular ion peak, which corresponds to the ligand formula weight, has peaks at m/z=280.00. The spectrum exhibited others peaks at (m/z) (190.01, 123.32, 92.04 and 70.01). The pattern for these peaks corresponding with (C₁₀H₁₂N₃O⁺, C₆H₇N₂O⁺, C₆H₆N⁺, C₄H₈N⁺and C₅H₇⁺). Fig 4 displays the mass spectrum of the Pt(IV) complex ,the pattern of

fragmentation is summarized in scheme3.The molecular ion peak, which corresponds to the ligand formula weight, has peaks at m/z=599.01, and other peaks at (m/z) (453.88, 435.18 ,329.77,144.08 and 134.27) might be related to (C₆H₆ClN₃O₂Pt⁺, C₅H₄N₃Cl₃OPt⁺, C₆H₄N₃OPt⁺, C₁₀H₁₀N⁺and C₆H₄N₃O⁺) respectively. Fig 5 displays the mass spectrum of the Au(III) complex, the pattern of fragmentation is summarized in scheme4. The molecular ion peak, which corresponds to the ligand formula weight, has peaks at m/z=547.11, and other peaks at (m/z) (346.11, 241.01, 130.15 and 108.44) might be related to (C₇H₇N₃AuO⁺, CH₄N₂Au⁺, C₉H₈N⁺and C₆H₆NO⁺) respectively ¹⁵⁻¹⁷.

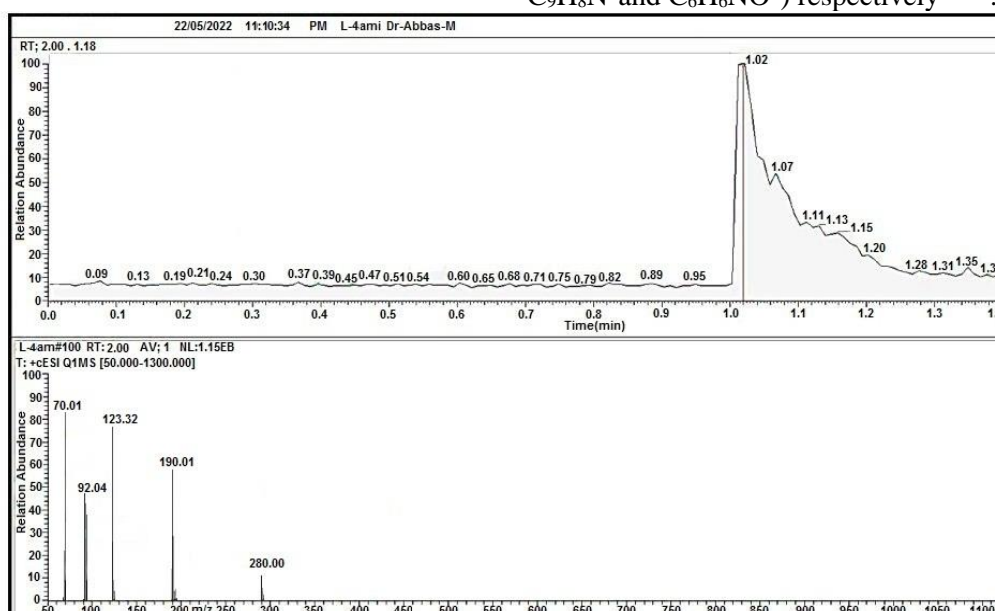


Figure 3. Mass spectrum of ligand

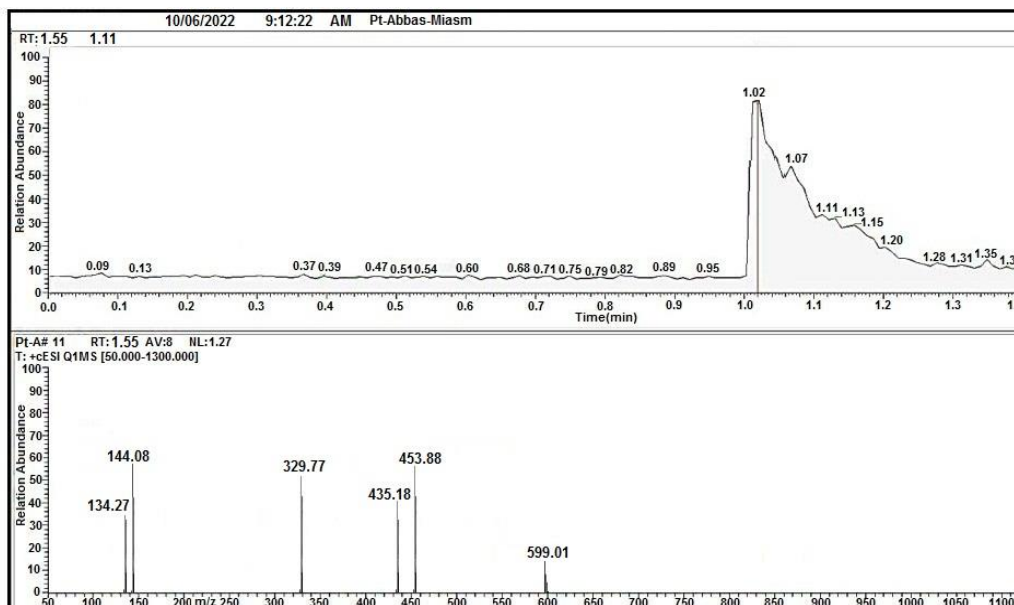


Figure 4. Mass spectrum of $[Pt(H_2L)(H_2O) Cl_3]$

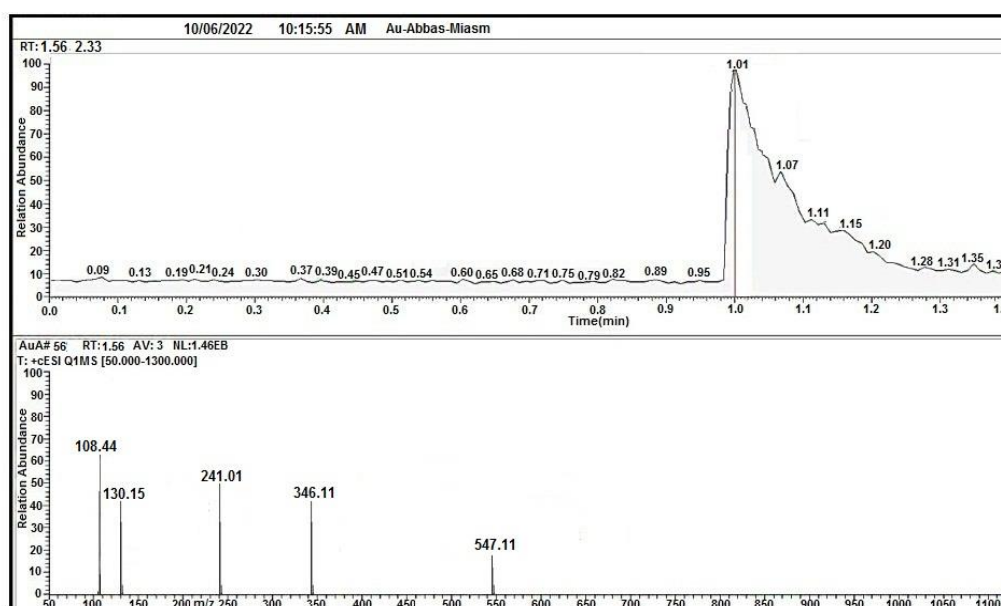
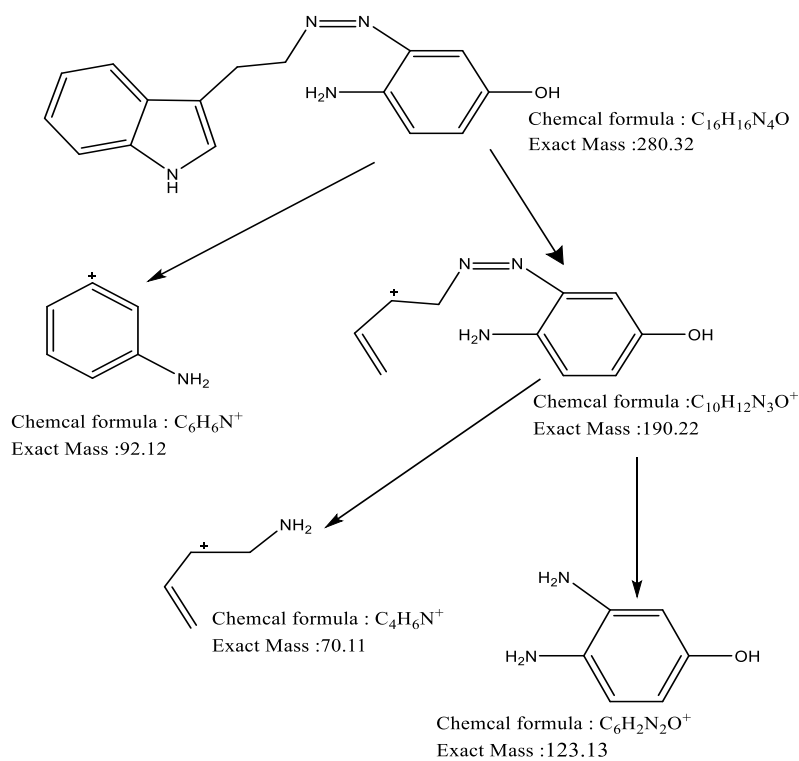
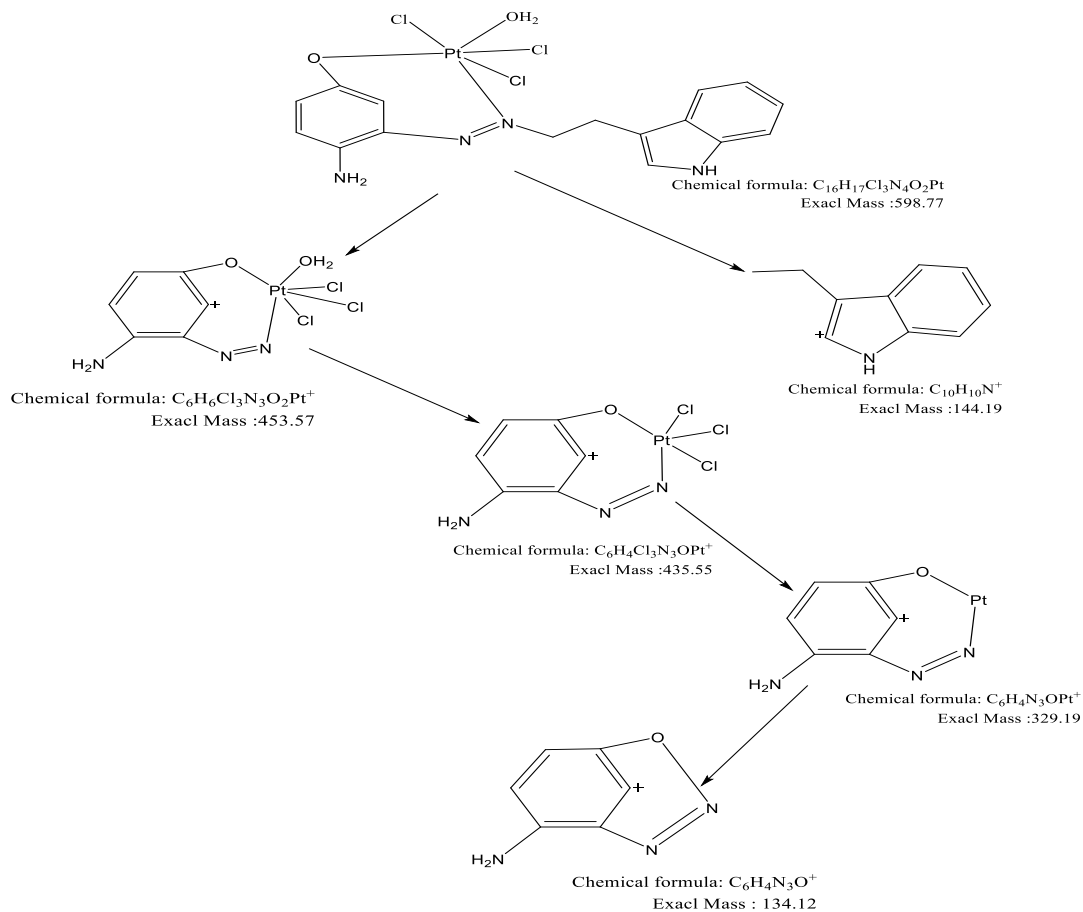


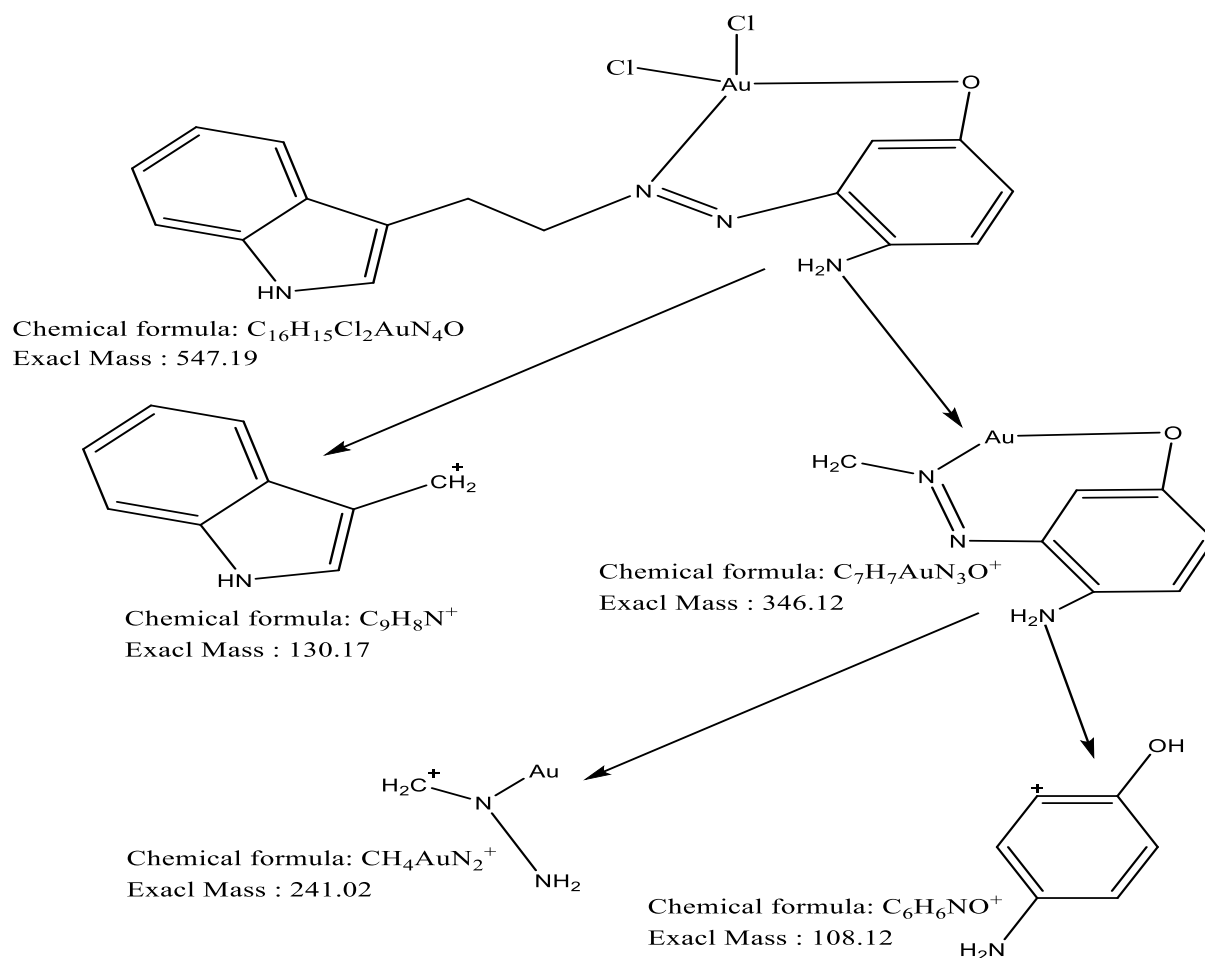
Figure 5. Mass spectrum of $[Au(H_2L) Cl_2]$



Scheme 2. Pattern of fragmentation of ligand H_2L



Scheme 3. Pattern of fragmentation for $[Pt(H_2L)(H_2O) Cl_3]$



Scheme 4. Fragmentation pattern for $[Au(H_2L) Cl_2]$

UV-Visible of Ligand (H_2L) and Their Metal Complexes

The electronic spectrum for ligand (H_2L) exhibited strong absorption at 258,363nm that belongs to ($\pi \rightarrow \pi^*$), ($n \rightarrow \pi^*$) respectively^{18,19}, Fig 6. The electronic spectrum for Ni(II) complex showed four peaks at 263, 411, 637 and 742 nm that are attributed to ($\pi \rightarrow \pi^*$), ($M \rightarrow LC.T$), $^3A_{2g} \rightarrow ^3T_{2g}$, $^3A_{2g} \rightarrow ^3T_{1g}$, and $^3A_{2g} \rightarrow ^3T_{1g_p}$ respectively. The Pd(II) complex electronic spectra displayed four peaks at (298, 368, 575, and 684) nm, which are attributed to transitions of types ($\pi \rightarrow \pi^*$), ($M \rightarrow L$ C. T), ($^1A_{1g} \rightarrow ^1B_{1g}$), ($^1A_{1g} \rightarrow ^1A_{2g}$) respectively²⁰⁻²², as shown Fig 7. The peaks at 273 and 391 nm are

ascribed to $\pi \rightarrow \pi^*$ and ($M \rightarrow LC.T$). In addition, two new absorption peaks at (466 and 587) nm are attributed to transitions type $^1A_{1g} \rightarrow ^1T_{2g}$, $^1A_{1g} \rightarrow ^1T_{1g}$, respectively of Pt(IV) complex. The electronic spectrum of the electronic absorption of Au (III) complex peaks at (241,301) nm attributed to the ($\pi \rightarrow \pi^*$), ($M \rightarrow L$), and (434) nm, (600) nm are attributed to the $^1A_{1g} \rightarrow ^1B_{1g}$, $^1A_{1g} \rightarrow ^1A_{2g}$, respectively. Showing that the Ni(II) and Pt(IV) complexes have an octahedral geometry, the square planar of both Pd(II) and Au(III) complexes²²⁻²³. Table 3 lists all the information on the electronic spectra.

Table 3. The UV-Vis spectra, magnetic moments and molar conductivity for ligand (H₂L) and their metal complexes

Comp.	Wave number		ABS	Assignment	μ eff BM	Suggested Structure	Λ_m cm ² $\Omega^{-1}mol^{-1}$
	(nm)	(cm ⁻¹)					
H ₂ L	258	38759.6	0.96	$\pi \rightarrow \pi^*$	-	-	-
	363	27548.2	1.52	n $\rightarrow\pi^*$ C.T L \rightarrow L			
[Ni(H ₂ L)(H ₂ O) ₃ Cl]	263	38022.8	1.51	$\pi \rightarrow \pi^*$	3.37	octahedral	13
	411	24330.9	0.94	$^3A_{2g} \rightarrow ^3T_{2g}$			
	637	15698.5	0.11	$^3A_{2g} \rightarrow ^3T_{1g}$			
	742	13477.0	0.16	$^3A_{2g} \rightarrow ^3T_{1g_p}$			
[Pd(H ₂ L)(H ₂ O) Cl]	269	37174.7	1.40	$\pi \rightarrow \pi^*$	diamagnetic	square planer	9
	358	27932.9	0.90	M \rightarrow L C. T			
	463	21598.2	0.52	$^1A_{1g} \rightarrow ^1B_{1g}$			
	584	17123.2	0.31	$^1A_{1g} \rightarrow ^1A_{2g}$			
[Pt(H ₂ L)(H ₂ O) Cl ₃]	273	36630.0	0.32	$\pi \rightarrow \pi^*$	diamagnetic	octahedral	17
	391	25575.4	0.46	M \rightarrow L C. T			
	466	21459.2	0.14	$^1A_{1g} \rightarrow ^1T_{2g}$			
	587	17035.7	0.21	$^1A_{1g} \rightarrow ^1T_{1g}$			
[Au(H ₂ L) Cl ₂]	241	41493.7	0.56	$\pi \rightarrow \pi^*$	diamagnetic	square planer	13
	301	33222.5	0.71	M \rightarrow L C. T			
	434	23041.4	0.31	$^1A_{1g} \rightarrow ^1B_{1g}$			
	600	16666.6	2.21	$^1A_{1g} \rightarrow ^1A_{2g}$			

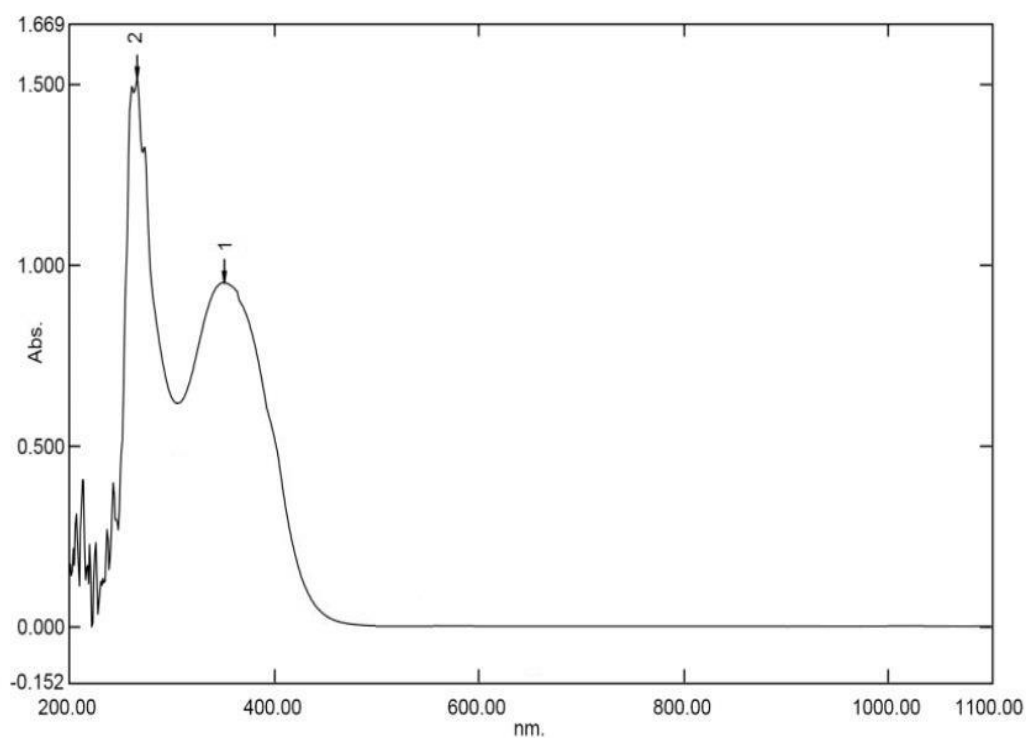


Figure 6. Electronic spectra of ligand (H₂L)

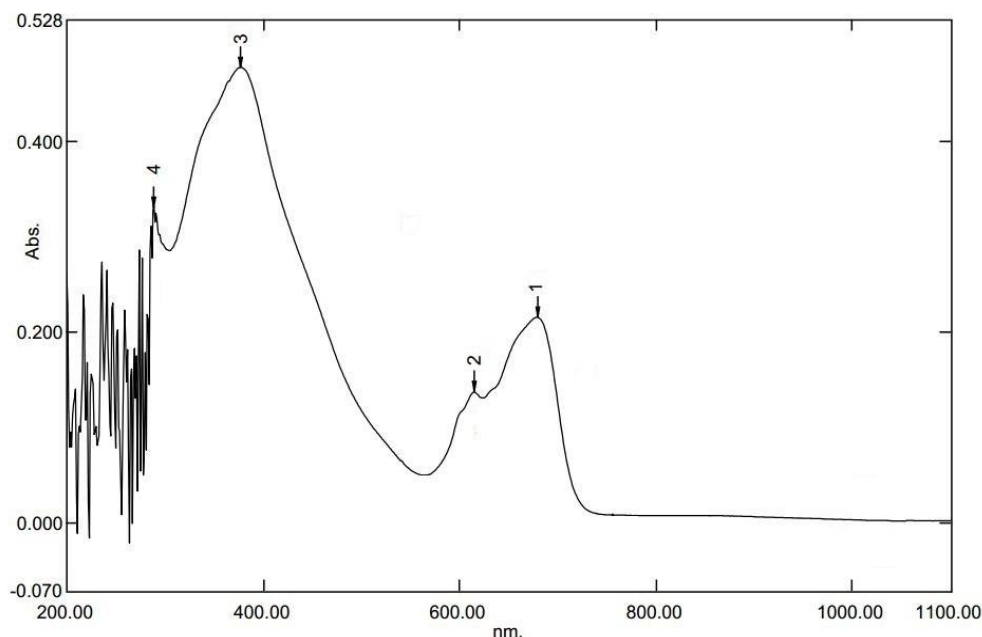


Figure 7. Electronic spectra of Pd (II)

Infrared Spectra

The functional groups of molecules, especially organic ones, that contain the donor atom when coordination occurs were identified using FTIR data^{24,25}. Strong absorption bands at 3500 cm^{-1} and 3241 cm^{-1} that correspond to the (O-H), (NH) indole ring, respectively, and the band at 1461 cm^{-1} that is related with the novel azo group (N=N) are all found in the FTIR spectrum of the ligand (H_2L) shown in Fig. 8.²⁵⁻²⁷ Infrared complexes are found, and their spectra are contrasted with the spectrum of a free ligand to identify any differences. When compared to the ligand spectrum, all complex spectra show the elimination of the (O-H) phenolic and the shifted azo group (N=N). This demonstrates that the

ligand and metal ion were coordinated via the nitrogen and oxygen atoms as well as via the nitrogen of the azo group²⁸. In addition, new bands have been observed that belong to (M-N) at (593, 585, 562, and 554) cm^{-1} for the complexes of Ni, Pd, Pt, and Au, respectively, and (M-O) at (514, 521, 527, and 489) cm^{-1} for the complexes Ni, Pd, Pt, and Au, respectively, supporting the occurrence of coordination through the nitrogen and oxygen atoms²⁹⁻³¹. Ni(II) complex as shown in Fig 9. Every complex's new bands were discovered to correlate with its coordinated water molecules³². Table 4 lists the ligand's distinctive vibrations and assignments, along with those of its complexes.

Table 4. The IR spectra bands (cm^{-1}) for ligand (H_2L) and their metal complexes

Compounds	ν (OH)	ν ($\text{NH}_{2\text{sym}}$) ν (NH_{asym})	ν ($\text{NH}_{\text{indole}}$)	ν (C-H) arom.	ν (C-H) aliph.	ν (N=N)	ν (H_2O) aqua	ν (M-N)	ν (M-O)
H_2L	3500	3411 3375	3241	3041	2977	1461	-	-	-
$[\text{Ni}(\text{H}_2\text{L})(\text{H}_2\text{O})_2]$	-	3435 3407	3244	3085	2982	1472	3740 1636 835	593	514
$[\text{Pd}(\text{H}_2\text{L})(\text{H}_2\text{O})\text{Cl}]$	-	3437 33224	3137	3087	2978	1447	3756 1602 824	585	521
$[\text{Pt}(\text{H}_2\text{L})\text{Cl}_3(\text{H}_2\text{O})]$	-	3453 3509	3289	3048	2878	1487	3736 1602 824	562	527
$[\text{Au}(\text{H}_2\text{L})\text{Cl}_2]$	-	3403 3358	3286	3095	2978	1474	-	554	489

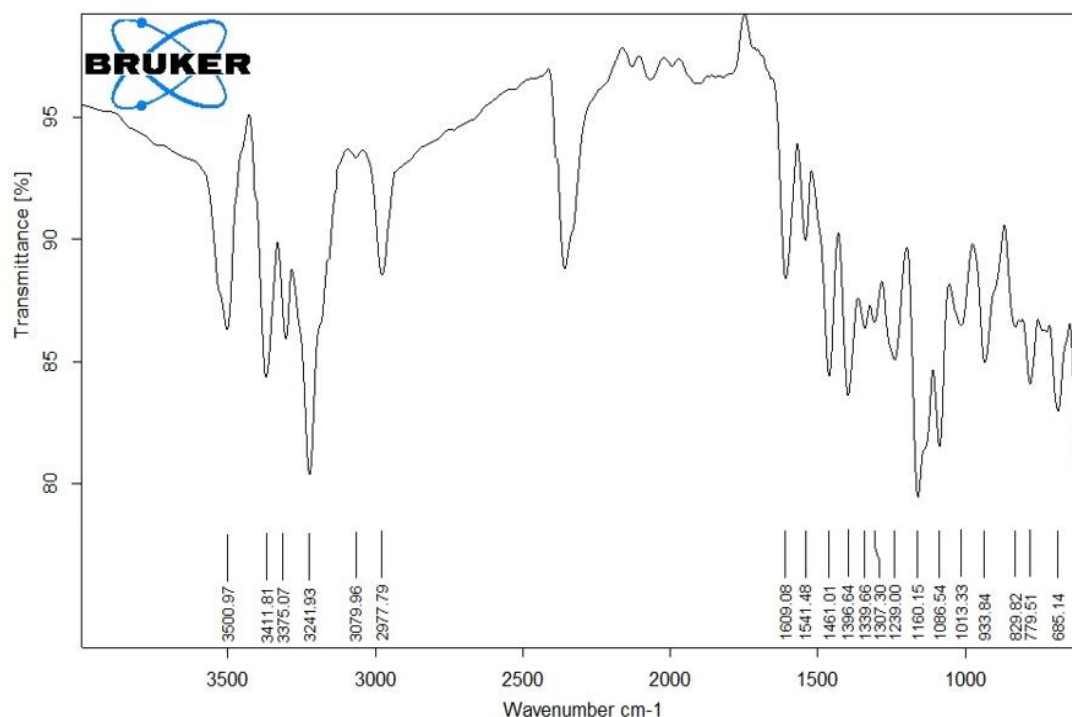


Figure 8. FT-IR Spectra for ligand (H₂L)

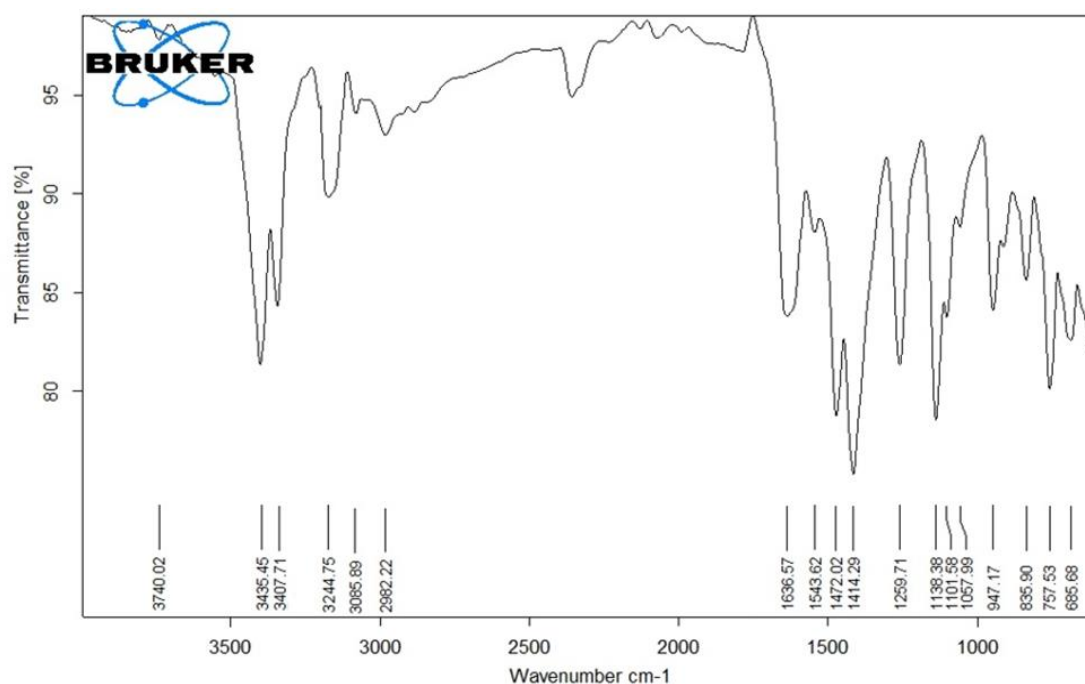


Figure 9. FT-IR Spectra for [Ni(H₂L)(H₂O)₃Cl]

Thermal Study Data

The findings of the thermal analysis for ligand (H₂L) and their synthesized complexes are displayed in Tables 5,6, and Figs. 10, 11 respectively. Tentative decomposition reaction of metal complexes are summarized in schemes 5.

Decomposition stages, temperature ranges, decomposition products, and weight loss complex percentages were computed based on the thermograms, and they showed agreement. Between their thermal decomposition results and calculated values, that validates elemental analysis results and

suggested equations^{33,34}. In this work, it was noted that the remaining ligand was carbon and the remaining metal oxide in the ligand and metal complexes of Pd(II) and Au(III). According to the

results of the thermo gravimetric tests, the complexes and the ligand decompose in (one to three) phases. The thermodynamic parameters ΔH , ΔS and ΔG were computed using the DCS curve.

Table 5. TGA data of the ligand (H₂L) and synthesized complexes

Comp.	T _i °C	T _f °C	T Max	ΔH J/g	ΔS J	ΔG J	Type
H ₂ L	41.08	106.52	55.81	-37.45	-0.57	0.784	exo
	127.85	172.88	150.79	-17.08	-0.37	40.11	exo
	182.36	196.21	189.75	-1.119	-0.085	15.11	exo
	218.64	305.41	254.77	238.78	2.75	371.83	endo
[Pd(H ₂ L)(H ₂ O)Cl]	387.65	395.13	392.40	-3.03	-0.40	153.93	exo
[Au(H ₂ L) Cl ₂]	70.38	119.40	99.40	-115.03	-2.34	18.73	exo
	127.48	188.10	157.80	-222.66	-3.68	556.46	exo
	204.48	227.99	215.11	-9.22	-0.40	76.93	exo
	230.45	286.67	251.01	-50.47	-0.89	174.86	exo

endo: endothermic, exo: exothermic

Table 6. DSC data of the ligand (H₂L) and their complexes

Comp.	T _i C°	T _f C°	T max	%Estimated (calculated)		Assignment
				mass loss	Total Mass loss	
H ₂ L	201.1	349.34	284.33	43.532	99.463	-H ₂ O
	349.34	593.80	468.31	(43.164)	(99.884)	-C ₁₆ H ₁₅ N ₄ Cl
				55.931 (56.720)		-C ₆ H ₉ N ₃ C
[Pt(H ₂ L)(H ₂ O) Cl ₃]	40.34	100.50	74.31	3.080	66.281	-2H ₂ O
	100.50	207.47	162.21	(3.006)	(67.388)	-Cl
	207.47	349.75	280.33	5.897		-Cl ₂
	349.75	593.80	478.21	(5.928)		-C ₁₆ H ₁₅ N ₄ O
			11.532 (11.857)			PtO
			45.771 (46.595)			
[Au(H ₂ L) Cl ₂]	201.22	333.66	278.33	18.379	61.775	-Cl
	333.66	595.54	470.44	(18.092)	(61.039)	-N ₂
				43.298 (42.946)		-C ₁₆ H ₁₅ N ₂ AuO

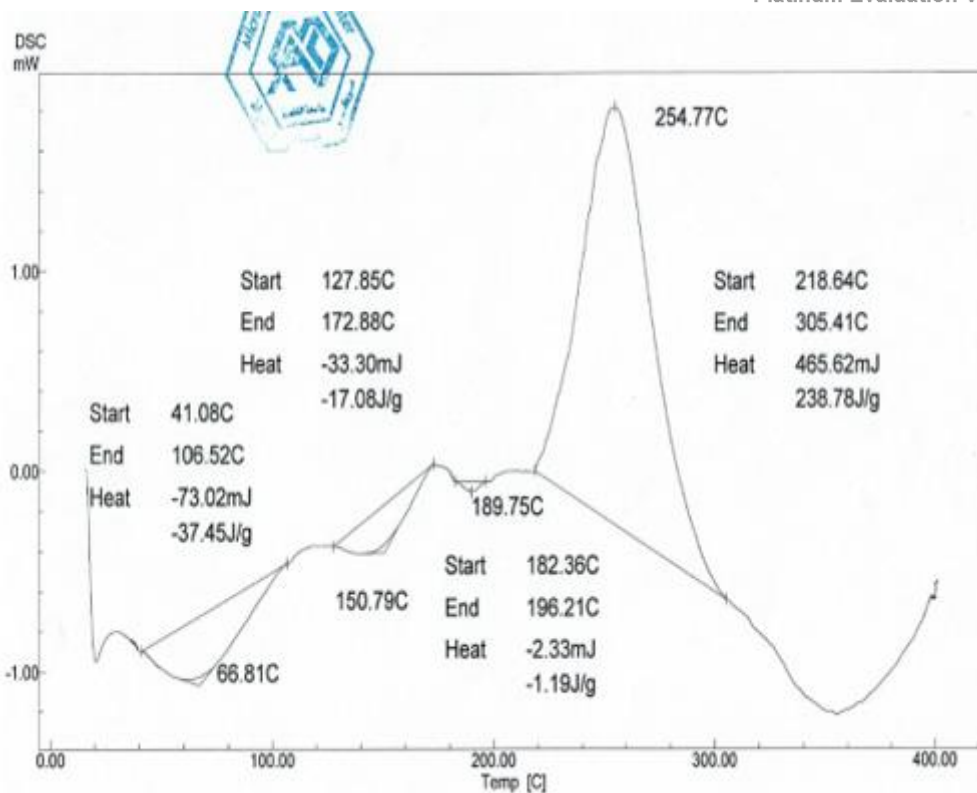
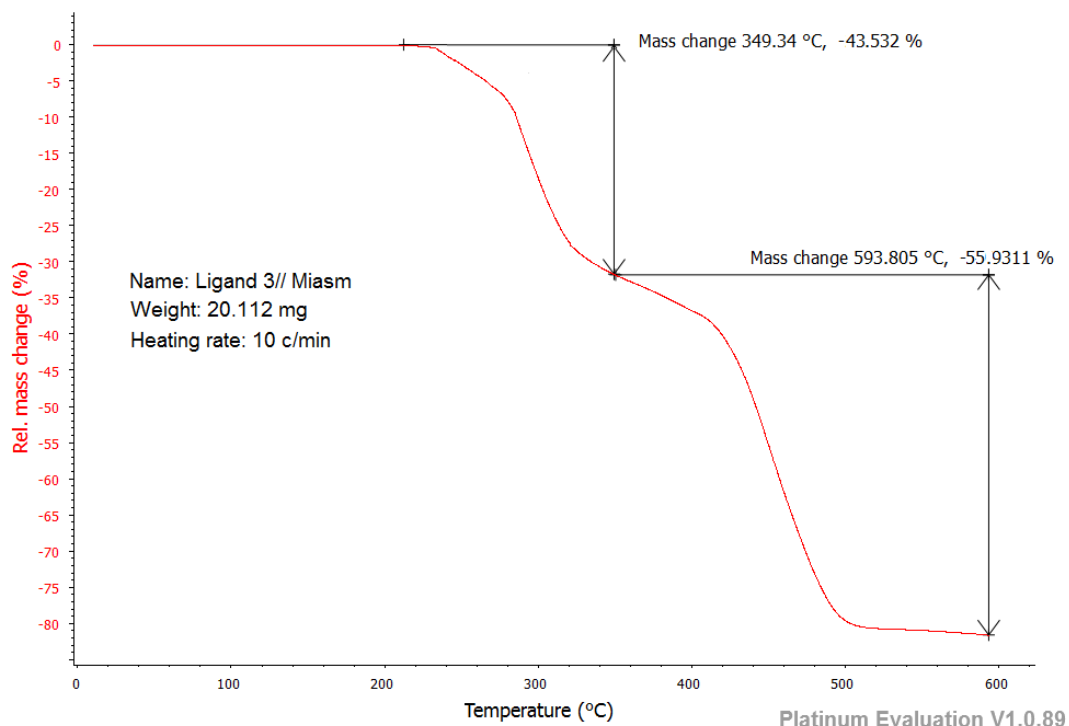


Figure 10. Thermo gravimetric Ligand

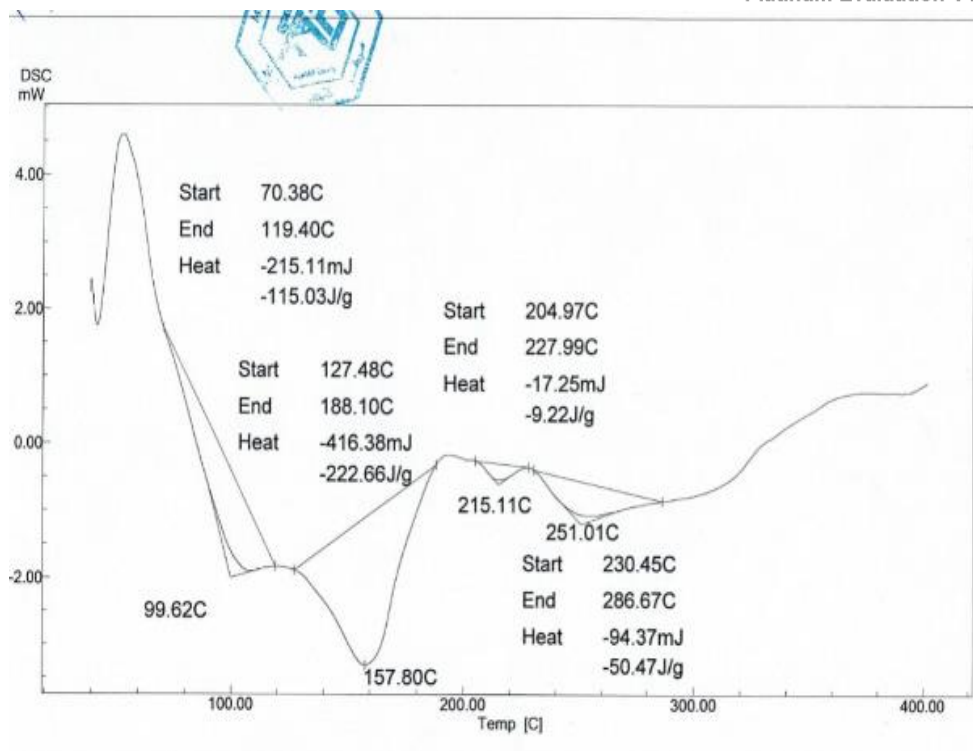
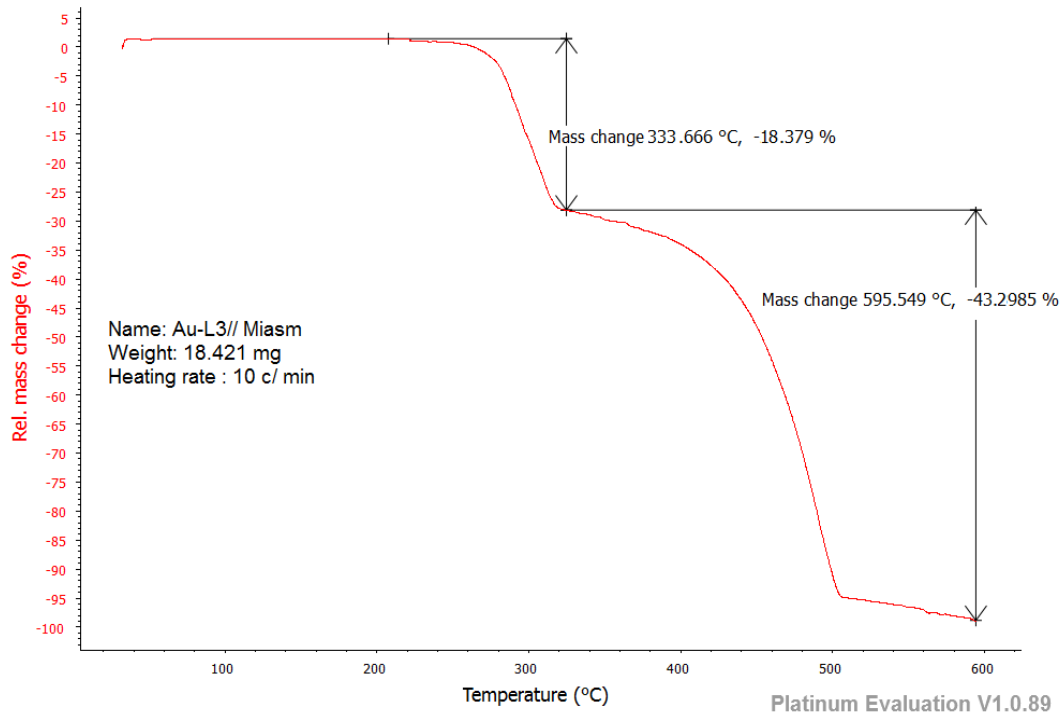
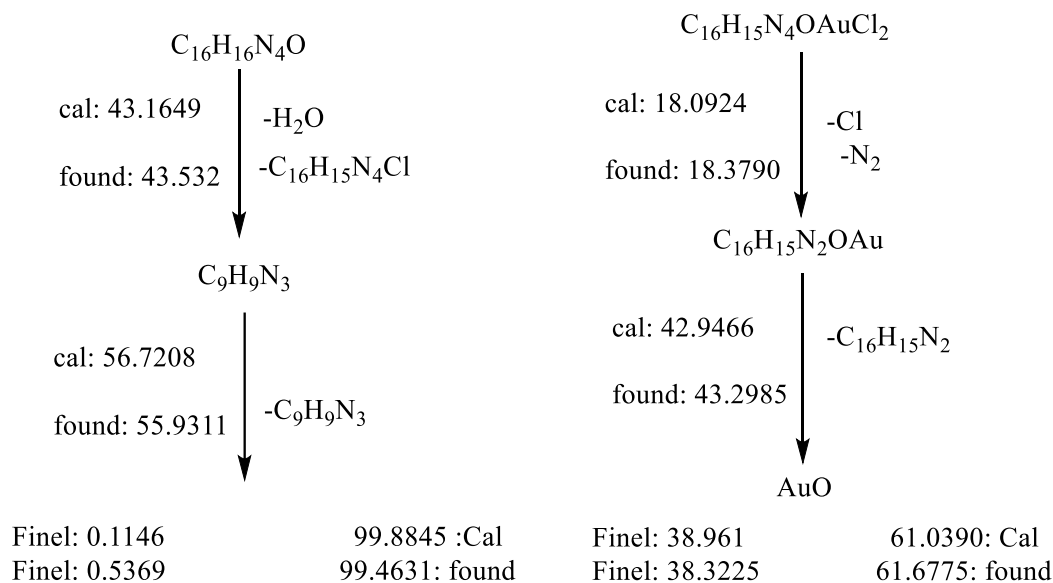


Figure 11. Thermo gravimetric Au(III) complex



Scheme 5. Tentative decomposition reaction of metal complexes

Antioxidant Activity

The majority of studies use the DPPH method to determine the action as an antioxidant of ligands and their metal complexes because of the straightforward methodology and high reliability³⁵. Ligand (H₂L) and synthesized complexes Ni(II), Pd(II), Ptt(IV) and Au (III) their radical-scavenging

activity were assessed by DPPH after the reduction, DPPH reacts with the ligand and the color of DPPH changes from purple to yellow³⁶, the Pd (II) exhibited better scavenging activity at 30 minute, while Au(III) complex exhibited least scavenging activity to compare gallic acid (standard). The results of all test of compounds were averaged and are listed in Table7.

Table 7. Means, standard deviations, coefficients of variation, Correlation coefficient and IC₅₀ of antioxidant activity in percentage (aa%) of the tested samples of ligand (H₂L) at 30 minute.

Tested sample	Mean	Standard deviation	Coefficient of variation%	Correlation coefficient	IC ₅₀
Gallic acid	44.491	2.667815	2.446236	0.996263	-5.4431
H ₂ L	82.319	2.378803	7.071362	0.993625	0.1352
[Ni(H ₂ L)(H ₂ O) ₃ Cl]	89.835	3.678135	3.336549	0.993302	-0.1578
[Pd(H ₂ L)(H ₂ O)Cl]	83.625	1.666317	2.136768	0.988885	-4.6395
[Pt(H ₂ L)(H ₂ O) Cl ₃]	69.016	2.531241	3.666783	0.977653	-0.7935
[Au(H ₂ L) Cl ₂]	74.436	1.351342	5.345487	0.993677	1.0453

IC₅₀ (the 50% maximum inhibitory concentration)

Conclusion

In summary, we successfully synthesized a new Azo ligand derivatives of tryptamine 3-((2-(1H-indol-2-yl)ethyl)diazinyl)-4-aminophenol by simple substitution reaction from tryptamine with 4-aminophenol. Then we characterized ligand and metal complexes by various analytical techniques, like elemental microanalysis, metal – chloride containing, electrical conductivity measurement, magnetic susceptibility, ¹H and ¹³CNMR, FT-IR, UV-Vis, mass spectra, and thermal analysis (TGA and DSC) curves. The DCS curve was used to

calculated the thermodynamic parameters ΔH, ΔS, and ΔG. The yield of the synthesized compounds was found to be in the range from 60-80%. The molar conductivity results showed that none of the produced complexes are electrolytes, and the atomic N and O coordination sites in the ligand were identified by comparing their IR spectra to those of the metal complexes. The M:L ratio in every compound was [1:1]. According to the results, octahedral geometry suggest of Ni(II) and Pt(IV) complexes, Pd(II) and Au(III) complexes' square

planar. Antioxidant activity of the synthetic compounds were evaluated against the DPPH radical (1,1-diphenyl-2-picrylhydrazyl), and the results were

contrasted with those of gallic acid, a widely used natural antioxidant. Results showed how efficient metal complexes was at scavenging free radicals.

Author's Declaration

- Conflicts of Interest: None.
- We hereby confirm that all the Figures and Tables in the manuscript are ours. Furthermore, any Figures and images that are not ours have been included with the necessary permission for

re-publication, which is attached to the manuscript.

- Ethical Clearance: The project was approved by the local ethical committee in University of Baghdad.

Author's Contribution Statement

M. Q. A. and A. A. S. conceived, planned and carried out the experiments and the simulations. All the authors contributed to sample preparation, contributed to the interpretation of the results and

took the lead in writing the manuscript. The authors provided critical feedback and helped shape the research, analysis, and revision of manuscript.

References

1. Suleman VT, Al-Hamdani AAS, Ahmed SD, Jirjees VY, Khan ME, et. al. Phosphorus Schiff base ligand and its complexes: Experimental and theoretical investigations. *Appl Organomet Chem.* 2020; (34)4: e5546. <https://doi.org/10.1002/aoc.5546>
2. Hamza IS, Mahmmoud WA, Al-Hamdani AAS, Ahmed SD, Allaf AW, Al Zoubi W. Synthesis, characterization, and bioactivity of several metal complexes of (4-Amino-N-(5-methyl-isaxazol-3-yl)-benzene sulfonamide). *Inorg Chem Commun.* 2022; 14(4): 109776. <https://doi.org/10.1016/j.inoche.2022.109776>
3. Obaid SMH, Jarad AJ, Al-Hamdani AAS. Synthesis, Characterization and Biological Activity of Mixed Ligand Metal Salts Complexes with Various Ligands. *J Phys Conf Ser.* 2020; 20(1): 012028. <https://doi.org/10.1088/1742-6596/1660/1/012028>
4. Rana AK, May MJA, Tagreed NAO. Synthesis, Characterization and Antimicrobial Evaluation of New Azo Compounds Derived from Sulfonamides and Isatin Schiff Base. *Int J Drug Deliv Technol.* 2020; 10(1): 150-155. <https://doi.org/10.25258/ijddt.10.1.22>
5. Hasan M. Synthesis, Identification, and Biological Study for Some Complexes of Azo Dye Having Theophylline. *Sci World J.* 2021; 76(3): 1-9. <https://doi.org/10.1155/2021/9943763>
6. Al-Hamdani AAS, Abdel MB, Ahmad F, Shayma AS. New Azo-Schiff Base derived with Ni(II), Co(II), Cu(II), Pd(II) and Pt(II) complexes: preparation, spectroscopic investigation, structural studies and biological activity. *J Chil Chem Soc.* 2015; 60(1): 2774-2785. <http://dx.doi.org/10.4067/S0717-97072015000100003>
7. Moamen SR, AltalhiT., Safyah BB, Ghaferah HA and Kehkashan A. New Cr(III), Mn(II), Fe(III), Co(II), Ni(II), Zn(II), Cd(II),and Hg(II) Gibberellate Complexes: Synthesis, Structure, and Inhibitory Activity Against COVID-19 Protease. *Russ J Gen Chem.* 2021; 91(5): 890 - 896. <https://doi.org/10.1134/S1070363221050194>
8. Jirjees VY, Al-Hamdani AAS, Wannas NM, A. RF, Dib A, Al Zoubi W. Spectroscopic characterization for new model from Schiff base and its complexes. *J Phys Org Chem.* 2020; (34)4: e4169. <https://doi.org/10.1002/poc.4169>
9. Al-Hamdani AAS, Al Zoubi W. New metal complexes of N3 tridentate ligand: Synthesis, spectral studies and biological activity. *Spectrochim Acta A: Mol Biomol Spectrosc.* 2015; 137: 75-89. <https://doi.org/10.1016/j.saa.2014.07.057>
10. Al-Daffay RKH, Al-Hamdani AAS. Synthesis and Characterization of Some Metals Complexes with New Acidicazo Ligand 4-[(2-Amino-4-Phenylazo)-Methyl]-Cyclohexane Carboxylic Acid. *Iraqi J Sci.* 2022; 63(8): 3264-3275. <https://doi.org/10.24996/ij.s.2022.63.8.2>
11. Al-Daffay RKH, Al-Hamdani AAS. Synthesis, Characterization, and Thermal Analysis of a New Acidicazo Ligand's Metal Complexes. *Baghdad Sci J.* 2022; 19(3): 121-33. : <http://dx.doi.org/10.21123/bsj.2022.6709>
12. Al-Bahadili ZR, Al-Hamdani AAS, Rashid FA, Al-Zubaidi LA, Ibrahim SM. An Evaluation of the Activity of Prepared Zinc Nanoparticles with Extract of Alfalfa Plant in the Treatment of peptidase and ions in water. *Chem Methodol.* 2022 November; 19(6): 1399-1409. <https://doi.org/10.21123/bsj.2022.7313>

13. Al-Hamdani AAS, Zainab AAH. Spectroscopic Studies and Thermal Analysis of New Azo Dyes Ligands and their Complexes with some Transition of Metal Ions. *Baghdad Sci. J.* 2016; 13(3): 511-523. <https://doi.org/10.21123/bsj.2016.13.3.0511>
14. Kirill VY, Aleksandr SS, Werner K, Sergey AG. Synthesis, Crystal Chemistry of Octahedral Rhodium (III) Chloroamines. *bimol. Int J Corros.* 2020; 25(768): 1-17. <https://doi.org/10.3390/molecules25040768>
15. Samy ME, Moamen SR, Fawziah AA, Reham ZH. Situ Neutral System Synthesis, Spectroscopic, and Biological Interpretations of Magnesium (II), Calcium(II), Chromium(III), Zinc(II), Copper(II) and Selenium(IV) Sitagliptin Complexes. *Int. J. Environ. Res. Public Health.* 2021; 18(8030): 1-19. <https://doi.org/10.3390/ijerph18158030Al-Khazraji> AMA, Al Hassani RAM. Synthesis, Characterization and Spectroscopic Study of New Metal Complexes form Heterocyclic Compounds for Photostability Study. *Syst Rev Pharm.* 2020; 11(5): 535-555. [doi:10.31838/srp.2020.5.71](https://doi.org/10.31838/srp.2020.5.71)
16. Waheeb AS, Al-Adilee KJ. Synthesis, characterization and antimicrobial activity studies of new heterocyclic azo dye derived from 2-amino-4, 5-dimethyl thiazole with some metal ions. *Mater Today Proc.* 2021; 42(5): 2150-2163. <https://doi.org/10.1016/j.matpr.2020.12.299>
17. Ahmadi RA, Amani S. Synthesis, Spectroscopy, Thermal Analysis, Magnetic Properties and Biological Activity Studies of Cu(II) and Co(II) Complexes with Schiff Base Dye Ligands. *Molecules.* 2012; 17(6): 6434-6448. <https://doi.org/10.3390/molecules17066434>
18. Unnisa A, Abouzied AS, Baratam A, Lakshmi KC. Synthesis, characterization, computational study and in-vitro antioxidant and anti-inflammatory activities of few novel 6-aryl substituted pyrimidine azo dyes. *Arab J Chem.* 2020; 13(12): 8638-8649. <https://doi.org/10.1016/j.arabj.2020.09.050>
19. Blümich B, Blümich P. *Pauly Essential NMR*. 1st ed. Springer Nature Switzerland. 2019; 65(8): 304 -321. <https://doi.org/10.1007/978-3-030-10704-8>
20. Mohammed H. Synthesis, Identification, and Biological Study for Some Complexes of Azo Dye Having Theophylline. *Sci World J.* 2021; 99(4): 37-63. <https://doi.org/10.1155/2021/9943763>
21. Shaalan ND, Abdulwahhab S. Synthesis, characterization and biological activity study of some new metal complexes with schiff's bases derived from [o-vanillin] with [2-amino-5-(2-hydroxy-phenyl)-1,3,4-thiadiazole]. *Egypt J Chem.* 2021; 6(4): 40-59. <https://doi.org/10.21608/EJCHEM.2021.66235.3432>
22. Shaalan N. Preparation, Spectroscopy, Biological Activities and Thermodynamic Studies of New Complexes of Some Metal Ions with 2-[5-(2-Hydroxy-Phenyl)-1,3,4-Thiadiazol-2-Ylimino]-Methyl-Naphthalen-1-Ol], *Baghdad Sci J.* 2022; 1(9): 813-829. <https://orcid.org/0000-0002-2875-5056>
23. Abou-Elyazed AS, Mohamed IF, Hegazy M. Complementary Studies on the Electrochemical Behavior of Nano Copper Sulfate with Cefdinir Antibiotic (CFD). *J Mater Sci Eng.* 2020; 10(2): 32-41. <https://doi.org/10.5923/j.materials.20201002.02>
24. Silverstein RM, Webster FX, Kiemle DJ. *Spectrometric Identification of Organic Compounds*. 7th ed. J W. A. INC, 2005; 2(21): 87-93. <http://article.sapub.org/10.5923/j.materials.20201002.02.html>
25. Barrahi, M. Corrosion inhibition of mild steel by Fennel seeds (*Foeniculum vulgare* Mill) essential oil in 1 M hydrochloric acid solution. *Int J Corros.* 2019; 8(4): 937-953. <https://doi.org/10.17675/2305-6894-2019-8-4-9>
26. Selma B, Sedat SB. Cobalt (II) and Manganese(II) Complexes of Novel Schiff Bases, Synthesis, Characterization, and Thermal, Antimicrobial, Electronic, and Catalytic Features. *Adv Chem.* 2014; 2014; (506851): 1-12. <https://doi.org/10.1155/2014/506851>
27. Muslah SI, Alabdali AJ, Shaalan ND. Synthesis of Binuclear Complexes of Cu (II), Ni (II) and Cr (III) Metal Ions Derived from Di-Imine Compound as Biterminal Binding Site Ligand. *ANJS.* 2020; 23(4): 19-28. <https://anjs.edu.iq/index.php/anjs/article/view/2340>
28. Rasheed AM, Al-Bayati S, Al Hasani R. Synthesizing, Structuring, and Characterizing Bioactivities of. Cr (III), La (III), and Ce (III). Complexes with Nitrogen, Oxygen, and Sulphur donor bidentate Schiff base ligands. *Baghdad Sci J.* 2021; 18(4): 23-33. [https://doi.org/10.21123/bsj.2021.18.4\(Suppl.\).1545](https://doi.org/10.21123/bsj.2021.18.4(Suppl.).1545)
29. Zehra S, Mobin M, Aslam R. Corrosion Inhibitors for High Temperature in Oil and Gas Industries', in *Sustainable Corrosion Inhibitors I: Fundamentals, Methodologies, and Industrial Applications*. ACS Publications. 2021; 14(6): 223-246. <https://doi.org/10.1021/bk-2021-1403.ch011>
30. Kirill V Y, Aleksandr S S, Werner K, Sergey A G. Synthesis, Crystal Chemistry of Octahedral Rhodium (III) Chloroamines. *Molecules.* 2020; 25(768): 1-17. <https://doi.org/10.3390/molecules25040768>
31. Kareem MJ, Al-Hamdani AAS, Jirjees VY, Khan ME, Allaf AW and Al Zoubi W. Preparation, spectroscopic study of Schiff base derived from dopamine and metal Ni (II), Pd (II), and Pt (IV) complexes, and activity determination as antioxidants. *J Phys Org Chem.* 2020; 34(3): 1-15. <https://doi.org/10.21123/bsj.2022.7289>
32. Anubha S, Rajneesh S. Synthesis, Characterization and Biological Evaluation of Transition and Inner Transition Metal Complexes of Ligands Derived Schiff Base from 1-phenyl-2, 3-dimethyl-4-(4-aminopentan-2-one)-pyrazole-5-one and 2-aminophenol. *Oriental Chem.* 2012; 29(2): 589-595. <http://dx.doi.org/10.13005/ojc/290228>

33. Mohamed G, El-Gamel G, El-Dien N. Preparation, chemical characterization, and electronic spectra of 6-(2-pyridylazo)-3-acetamidophenol and its metal complexes. *Synthesis React. Inorg Met Org. Chem.* 2001; 3(19): 347-358. <https://doi.org/10.1080/00387010009350159>
34. Mahdi MA, Jasim LS, Mohamed MH. Synthesis, Spectral and Biological Studies of Co (II), Ni (II) and Cu (II) Complexes with New Heterocyclic Ligand Derived From Azo-Dye. *Syst Rev Pharm.* 2021; 1(12): 426-434. <https://doi.org/10.1080/00958970802226387>
35. Masoud MS, Sweyllam AM, Ahmed MM. Synthesis, characterization, coordination chemistry and biological activity of some pyrimidine complexes. *J Mol Struct.* 2020; 12(19): 128-612. <https://doi.org/10.1016/j.molstruc.2020.128612>
36. Samy ME, Moamen SR, Fawziah AA, Reham ZH. Situ Neutral System Synthesis, Spectroscopic, and Biological Interpretations of Magnesium (II), Calcium(II), Chromium(III), Zinc(II), Copper(II) and Selenium(IV) Sitagliptin Complexes. *Int. J. Environ. Res. Public Health.* 2021; 18(8030): 1-19. <https://doi.org/10.3390/ijerph18158030>

تحضير، تشخيص وفعالية كمضادات اكسدة لليكاند ازو جديد وبعض المعقدات الفلزية المشتقة من التريبتامين

مياسم قاسم عبدالرضا¹، عباس علي صالح الحمداني¹، افتخار احمد حسين²

¹قسم الكيمياء، كلية العلوم للبنات، جامعة بغداد، بغداد، العراق
²فرع الكيمياء الصيدلانية، كلية الصيدلة، جامعة الفراهيدي، بغداد، العراق

الخلاصة

تم تحضير ليكاند الأزو الجديد (H_2L) من تفاعل ملح ديازونيوم التريبتامين مع مركب 4-امينوفينول. ثم تشخيصه بواسطة التحليل الدقيق للعناصر الى جانب التقنيات الطيفية الاشعة (فوق البنفسجية والاشعة تحت الحمراء والرنين النووي المغناطيسي للبروتون والكربون وطيف الكتلة). معقدات النيكل الثنائي والبلاديوم الثنائي وبلاتين الرباعي والذهب الثلاثي حضر وشخص بواسطة استخدام الامتصاص الذري والتحليل الدقيق للعناصر بالإضافة إلى طرق الطيفية (الاشعة تحت الحمراء وطيف الكتلة والاشعة فوق البنفسجية بالإضافة إلى القياسات المغناطيسية وتوصيلية). ثم استخدام منحنيات TGA و DSC في تحديد الاستقرار الحرارية للمركبات. حساب الثوابت الترمودينميك باستخدام منحني DSC جميع المعقدات بنسبة (1:1) فلز -ليكاند ، التوصيلية المولارية بينت ان المعقدات ذات طبيعة غير الكتروليتية. أليكاند في المعقدات، وفق التقنيات اعلاه، شخصت وتم اقتراح معقد النيكل (II) ومعقد بلاتين (IV) ثماني السطوح اما معقد بلاديوم (II) ومعقد الذهب (III) الشكل مربع مستوي. استخدمت طريقة كبح الجذور الحرة بواسطة DPPH لتقدير فعالية كمضادات اكسدة ليكاند ومعقدات الفلزية. أظهرت المركبات قدرة على كبح الجذور الحرة

الكلمات المفتاحية: فعالية كمضادات اكسدة ، ليكاند ازو ، DPPH ، ثوابت الترمودينميك ، طيف الكتلة.